

Journal of Geophysical Research: Atmospheres

RESEARCH ARTICLE

10.1002/2014JD021698

Key Points:

- Record high (low) values of O₃ and ClO (T and HCl) in February 2009
- Low temperatures favored greater O₃ production and O₃/O ratio
- ClONO₂+ClO+HCl remained approximately constant

Correspondence to:A. Damiani,
alecarlo.damiani@gmail.com**Citation:**

Damiani, A., B. Funke, M. López Puertas, A. Gardini, T. von Clarmann, M. L. Santee, L. Froidevaux, and R. R. Cordero (2014), Changes in the composition of the northern polar upper stratosphere in February 2009 after a sudden stratospheric warming, *J. Geophys. Res. Atmos.*, 119, 11,429–11,444, doi:10.1002/2014JD021698.

Received 26 FEB 2014

Accepted 8 SEP 2014

Accepted article online 10 SEP 2014

Published online 3 OCT 2014

Changes in the composition of the northern polar upper stratosphere in February 2009 after a sudden stratospheric warming

Alessandro Damiani^{1,2}, Bernd Funke³, Manuel López Puertas³, Angela Gardini³, Thomas von Clarmann⁴, Michelle L. Santee⁵, Lucien Froidevaux⁵, and Raul R. Cordero¹

¹Physics Department, University of Santiago de Chile, Santiago, Chile, ²Now at Japan Agency for Marine-Earth Science and Technology, Yokohama, Japan, ³Instituto de Astrofísica de Andalucía, CSIC, Granada, Spain, ⁴Institute for Meteorology and Climate Research, Karlsruhe Institute of Technology, Karlsruhe, Germany, ⁵Jet Propulsion Laboratory, California Institute of Technology, Pasadena, California, USA

Abstract Variability in the chemistry of the upper stratosphere/lower mesosphere region has been analyzed focusing on high latitudes during the boreal winter in 2009 characterized by the strong sudden stratospheric warming (SSW) on 24 January. Data from Michelson Interferometer for Passive Atmospheric Sounding aboard Envisat and the Microwave Limb Sounder on Aura have been used to exemplify these changes. Record high (low) values of O₃ and ClO (temperature and HCl) for the winters of 2005–2012, coupled with a simultaneous enhancement of ClONO₂, have been observed in February 2009. This suggests that the very low temperatures favor a more effective ozone production and a greater O₃/O ratio. The latter is the main factor controlling active chlorine partitioning. Increases of ClO lead to high ClONO₂ concentrations in the upper stratosphere at high latitudes, where its photodissociation rate is smaller. Since this increase of ClONO₂ happens at the expense of HCl, the region of high ClONO₂ roughly coincides with the region of low HCl. Although this period was characterized by an elevated stratopause event, the investigated region was not influenced by the descent of mesospheric air rich in NO_x. Some limited enhancements in NO_x at ~1 hPa occurred at latitudes greater than 80°N after about 20 February, but they became consistent only in March. Intrusion of midlatitude air mostly occurred between the SSW and early February. Then, the sum of volume mixing ratios of ClONO₂+ClO+HCl remained approximately constant and close to the values of the other years. In contrast, it was up to 0.2 ppbv lower during the SSW period. These atypical chemical conditions occurred also in February 2006, but 2009 stands out for its long-lasting effects, which persisted until late March.

1. Introduction

Sudden stratospheric warmings (SSWs) are severe meteorological events that influence the middle atmosphere of the polar regions during the winter. They entail variations in temperature, wind, air circulation, and chemistry [e.g., Matsuno, 1971; Holton, 1983]. SSWs have been shown to affect the tropospheric circulation on seasonal time scales [Baldwin and Dunkerton, 2001]. In the light of recent findings according to which variations in the frequency and dynamical properties of SSWs could be sensitive to anthropogenic greenhouse gas emissions [e.g., Charlton-Perez et al., 2008], studying them is of great scientific interest.

Recently, several authors have shown changes in the dynamical and chemical structure of the atmosphere occurred at northern high latitudes during and after the strong SSW events of January 2004, 2006, and 2009 [e.g., Siskind et al., 2007; Manney et al., 2008a, 2008b, 2009; Winick et al., 2009; Damiani et al., 2010; Orsolini et al., 2010; Randall et al., 2006, 2009; Smith et al., 2009; Salmi et al., 2011; Funke et al., 2010, 2011; Gao et al., 2011; Sofieva et al., 2012]. During these major SSW events, the stratopause dropped in altitude, often entirely broke down, and then reformed at very high altitudes (the so-called elevated stratopause event [Siskind et al., 2007]). Therefore, it affected the temperature structure and trace gas distributions [Manney et al., 2008a, 2008b, 2009; Damiani et al., 2010]. These SSW events were followed in February by an upper stratospheric/mesospheric vortex recovery coupled with low planetary wave activity, increased (decreased) mesospheric (upper stratospheric) temperatures, and severe descent of air from the mesosphere to the stratosphere [Manney et al., 2009]. These years have been identified as “anomalous” in contrast with the “quiet” years [Smith et al., 2009; Damiani et al., 2010].

While ozone (O_3) changes at middle/low stratospheric altitudes are mainly driven by dynamics, variations in O_3 volume mixing ratio (VMR) in the upper stratosphere/mesosphere are expected to be anticorrelated with those in temperature. Indeed, photochemical processes usually determine the O_3 abundance in the upper stratosphere/mesosphere, and its relation with the temperature is explained by the fact that both the O_3 production and destruction reactions are temperature dependent [e.g., Sonnemann *et al.*, 2006]. This has been reported in many previous studies [e.g., Gille *et al.*, 1981; Rood and Douglass, 1985; Froidevaux *et al.*, 1989; Hauchecorne *et al.*, 2010; Damiani *et al.*, 2010; Sofieva *et al.*, 2012; Douglass *et al.*, 2012; Stolarski *et al.*, 2012]. Since also other atmospheric compounds (e.g., odd nitrogen, hydrogen, and chlorine species) and related catalytic cycles are differently sensitive to temperature changes, the strong temperature variations occurring during and after the SSW events represent an opportunity to investigate the variability of the chemistry of the polar atmosphere [Kvissel *et al.*, 2012; Sofieva *et al.*, 2012].

Damiani *et al.* [2010] reported mesospheric O_3 and hydroxyl radical (OH) changes during and after the SSW events for 2005–2009. A drop of the secondary and tertiary ozone maxima by 3–5 km [Smith *et al.*, 2009; Damiani *et al.*, 2010], a brief increase in the secondary ozone layer at the time of the SSW, later followed by prolonged decrease during the subsequent downwelling [Tweedy *et al.*, 2013] and a strong descent of dry air from the lower mesosphere into the upper stratosphere during the three anomalous winters have also been reported [Orsolini *et al.*, 2010]. Sofieva *et al.* [2012] showed that the SSW-induced temperature enhancement caused O_3 and NO_3 variations in the upper stratosphere, while changes in NO_2 were mainly linked to mixing of different air masses. Salmi *et al.* [2011] highlighted the descent of NO_x ($NO_2 + NO + N$) from about 80 to 50 km during the 2009 winter. Nevertheless, since NO_x did not reach the stratosphere before the final vortex breakdown, NO_x -related catalytic cycles did not impact O_3 at these altitudes. Furthermore, anomalous chlorine concentrations in the upper stratosphere were identified for both February 2006 and 2009 [Damiani *et al.*, 2012a].

The present study, based on satellite data from the Michelson Interferometer for Passive Atmospheric Sounding (MIPAS) and Microwave Limb Sounder (MLS) instruments, analyzes the changes in O_3 , chlorine nitrate ($CIONO_2$), hydrogen chloride (HCl), chlorine monoxide (ClO), and temperatures, which occurred in the upper stratosphere at northern polar latitudes in February 2009 after the strong 24 January SSW event. These results are then compared with the variations that occurred during the 2005–2012 winters.

2. Satellite Data Sets

MIPAS is a limb emission Fourier transform spectrometer aboard the European Environmental Satellite (Envisat) that measured profiles of trace species and temperature from July 2002 to April 2012 [Fischer *et al.*, 2008]. It was put in a Sun-synchronous orbit (98.55° inclination) at about 800 km altitude with a 10:00 A.M. LT equator crossing time. For the present study, we employed a data set produced under the nominal observation mode, which covers tangent altitudes from about 6 to 72 km with a vertical sampling of 2–3 km in the stratosphere and 3–5 km in the mesosphere. The retrieval of the gas profiles from the limb emission spectra in the midinfrared has been performed with the MIPAS level 2 processor jointly developed by the Institute of Meteorology and Climate Research (IMK) and the Instituto de Astrofísica de Andalucía (IAA) [von Clarmann *et al.*, 2003]. Here we focus mainly on V5R $CIONO_2$, O_3 , and temperature; moreover, CH_4 and NO_x profiles are also briefly introduced [Höpfner *et al.*, 2007; von Clarmann *et al.*, 2009]. The precision of the individual profile of MIPAS $CIONO_2$ ranges from 0.06 to 0.09 ppbv (or 9% to 40%), and its vertical resolution is 5–8 (12–14) km below (above) 2 hPa. The recommended upper limit for $CIONO_2$ profiles is approximately 50 km [von Clarmann *et al.*, 2009]. The altitude resolution of MIPAS O_3 as inferred from the averaging kernels is about 2.5–3.5 km. Uncertainties in spectroscopic parameters dominate its total error budget, and its precision varies between about 4 and 6% at the investigated altitudes [von Clarmann *et al.*, 2009].

The NASA EOS (Earth Observing System) MLS [Waters *et al.*, 2006] aboard the Aura satellite was put in a Sun-synchronous orbit (98° inclination) with a 1:45 P.M. LT equator crossing time in July 2004. It records the temperature and trace gas profiles between 82°S and 82°N by scanning the Earth's limb and measuring the microwave emission in different regions of the spectrum. The MLS vertical resolution depends on the considered species and usually ranges between 3 and 4 km in troposphere/stratosphere and 8 km in the mesosphere. In this work we used the MLS version 3.3 of ClO, HCl, O_3 , and temperature level 2 data.

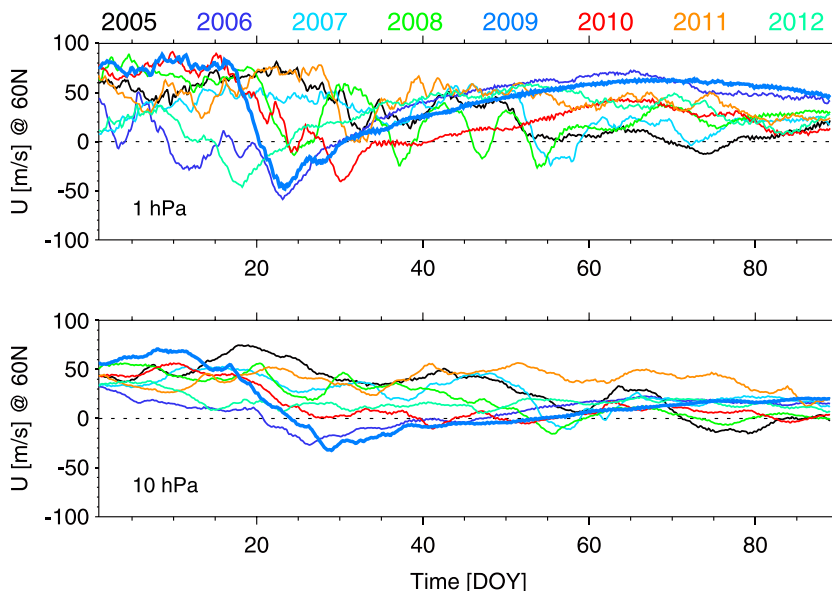


Figure 1. Zonal mean zonal wind from Modern Era Retrospective analysis for Research and Applications (MERRA) at latitude 60°N and (bottom) 10 hPa and (top) 1 hPa from January to the end of March for 2005–2012.

Validation studies of the version 2.2 MLS data products are presented in individual validation papers [Froidevaux *et al.*, 2008a, 2008b; Santee *et al.*, 2008; Schwartz *et al.*, 2008], while Livesey *et al.* [2011] summarized the differences between the version 2.2 and the current version 3.3. In the stratosphere, the precision of the single MLS CIO profile is about 0.1–0.3 ppbv (i.e., more than 50%) with systematic uncertainties lower than 15% [Santee *et al.*, 2008]. (Please note that the CIO VMRs in the upper stratosphere during February 2009 are more than double of the typical conditions (e.g., in 2005 or 2011). In this way, the increased signal-to-noise ratio allowed us to get information related to the upper stratosphere.) Its vertical resolution, as inferred from the averaging kernels, is about 3–4.5 km. Meaningful data are obtained in the region between 100 and 1 hPa. In the stratosphere and the lower mesosphere, the MLS HCl product has a precision of 0.2–0.7 ppbv (from 10% to 20%) and good accuracy (10%) [Froidevaux *et al.*, 2008a], and its vertical resolution is about 3 km. The vertical resolution for MLS O₃ data in the upper stratosphere/lower mesosphere (USLM) region is ~2.5–4 km with the better (poorer) resolution below (above) about 1 hPa. In the altitudinal region examined in this paper (i.e., 10–0.5 hPa), the precision of the individual O₃ profiles ranges from 0.1 to 0.3 ppmv, and the accuracy is about 5%.

3. Results

Recently, several works have carefully addressed the meteorological evolution of the northern polar vortex during the 2009 winter by using satellite observations (e.g., MLS/Aura, submillimeter radiometer/Odin, Atmospheric Chemistry Experiment-Fourier transform spectrometer), reanalysis (e.g., GEOS-5 and European Centre for Medium-Range Weather Forecasts (ECMWF)), and models (e.g., FinROSE) [e.g., Manney *et al.*, 2009; Randall *et al.*, 2009; Orsolini *et al.*, 2010; Salmi *et al.*, 2011]. Therefore, for the specific meteorological issues, we refer the reader to these studies. The major SSW, which occurred in January 2009, is considered one of the strongest and most prolonged SSWs on record and resulted in a split of the polar vortex [Manney *et al.*, 2009]. Its strong impact on the lower stratosphere prevented the vortex recovery at these altitudes while, after the reformation of an elevated stratopause at about 80 km, the upper stratospheric vortex recovered in February. During the recovery phase, a strong downward motion from the mesosphere to the upper stratosphere induced the descent of NO_x [Randall *et al.*, 2009] coupled with warm and dry air [Orsolini *et al.*, 2010] with high CO concentration [Damiani *et al.*, 2010]. In contrast, decreased temperatures peaking at 1 hPa characterized the USLM region in February 2009. The latter has been shown to be caused by a reduced downwelling around 1 hPa due to the weaker westward gravity wave forcing in the upper mesosphere [Tomikawa *et al.*, 2012].

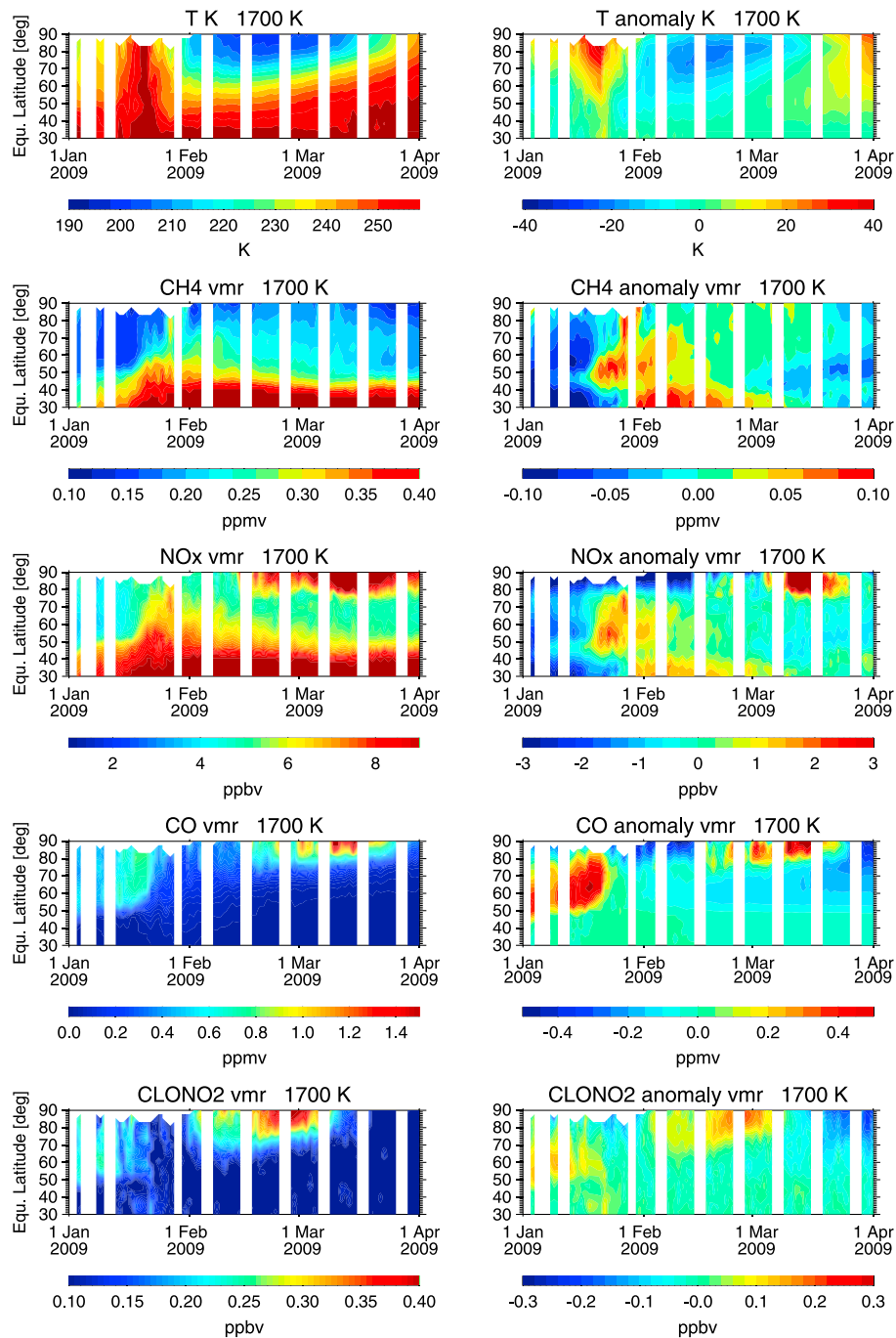


Figure 2. (top to bottom rows) Time-equivalent latitude distribution of (left column) MIPAS temperature, CH₄, NO_x, and CO values and (right column) differences with respect to the average of the January–March period on the 1700 K isentropic surface (about 1.5 hPa) for January–March 2009.

Figure 1 shows the zonal mean zonal wind from Modern Era Retrospective analysis for Research and Applications (MERRA, <http://gmao.gsfc.nasa.gov/research/merra/>) at latitude 60°N and 10 hPa and 1 hPa from January to the end of March for 2005–2012. After the SSW of January 2009, the polar wind at 10 hPa reverses to easterlies, and the vortex does not reform [e.g., Manney et al., 2009]. This is evident if we compare the time series of 2009 with quiet years (e.g., 2005 and 2011). In contrast, the zonal wind evolution in 2009 (as well as in 2006) at 1 hPa shows that after the polar wind reversal, westerlies regain strength during February and evolve together with simultaneously decreasing temperatures (see Figure 2). The zonal wind reversal to easterlies

inhibits the upward propagation of westward gravity waves. Therefore, in the absence of gravity wave drag, radiative cooling stimulates upper stratospheric/mesospheric vortex recovery, and the westerlies regain strength [e.g., Orsolini *et al.*, 2010, and references therein].

Figure 2 shows the time-equivalent latitude distribution of MIPAS temperature, CH₄, NO_x, and CO on the 1700 K isentropic surface (about 1.5 hPa) for January–March 2009. Equivalent latitudes have been calculated from data of potential vorticity from the European Centre for Medium-Range Weather Forecasts (ECMWF) as in Nash *et al.* [1996]. Soon after the SSW event of January 2009, temperature changes are evident from low to high latitudes. Then, the pattern evolves constraining temperature changes to only middle-high latitudes in late February and March. After the SSW event, the temporal evolution of CH₄ shows an ingress of midlatitude air characterized by high CH₄ VMRs to the polar vortex, followed by lower CH₄ values in February. Nevertheless, in February, the horizontal gradient of the CH₄ is weaker than during the pre-SSW period. The distribution of NO_x indicates a limited contribution from low-latitude air to the NO_x budget in the polar vortex soon after the SSW, with values remaining roughly constant in the region 50–75°N during the following period. On the contrary, at very high latitudes, the temporal evolution of the NO_x presents a small enhancement starting around 20 February which becomes intense in March. The mesospheric origin of this enhancement has been previously reported [e.g., Randall *et al.*, 2009; Salmi *et al.*, 2011], and it is evident in Figure 3a. Moreover, the descent of mesospheric air is easily recognizable also in the CO pattern (Figure 2, bottom row). It shows higher CO VMRs confined to the polar vortex before the SSW, very low values between the SSW and about 20 February, and a new enhancement, limited to very high latitudes, which gradually increases during the following period.

Figures 3a and 3b present the temporal evolution of zonal mean values and anomalies (computed with respect to the average of the January–March period) in the USLM region in MIPAS temperature, CH₄, O₃, NO_x, and ClONO₂ at 70–90°N and in MLS HCl and ClO at 70–82°N for January–March 2009 and 2011, respectively. The anomalous atmospheric conditions during the 2009 winter are evident. After the strong temperature enhancement that occurred during the SSW of 24 January 2009, an intense temperature decreases, most pronounced at 1 hPa, occurred in February. Elevated CH₄ values starting after the SSW and lasting throughout February are indicative of the intrusion of middle-latitude air at high latitudes after the vortex split [e.g., Manney *et al.*, 2009]. High O₃ VMRs are evident around 1 hPa in February, when ozone reaches record values for 2005–2012. Moreover, while the usual inner-polar vortex descent of NO_x is interrupted in February, NO_x seems to reach again upper stratospheric altitudes from mid-March on. Moreover, it is interesting to note that during the second half of February, low NO_x values coincide with high upper stratospheric O₃. It clearly shows that the NO_x of mesospheric origin did not impact the ozone budget in February. Finally, the transient enhancement in ClONO₂ at 1–2 hPa in February cannot be directly linked to dynamics. It could imply variations in the chlorine partitioning followed by ClONO₂ photolysis due to the increasing springtime sunlight in March [von Claramann *et al.*, 2013].

These conditions contrast with those of 2011 (Figure 3b). During the cold winter in 2011, the anomalously strong Arctic stratospheric vortex was the most isolated ever observed, and this resulted in a large volume of polar stratospheric clouds. Indeed in February–March 2011, the transport barrier at the Arctic vortex edge was the strongest in the last 30 years, and the persistence of a strong, cold vortex from December through to the end of March was unprecedented [Manney *et al.*, 2011]. These conditions enabled severe ozone depletion in late winter [Sinnhuber *et al.*, 2011] and preserved the usual inner-polar vortex air descent. In this way, the winter in 2011 can be considered a quiet year in contrast with 2009. Indeed, striking differences with respect to 2009 are apparent. The distribution of temperatures and CH₄ in the USLM region roughly remains uniform pointing to the absence of strong variability related to SSW events. In January, the NO_x descent from the mesosphere to the upper stratosphere is larger compared with the same period of the 2009. Moreover, in contrast with 2009, there is no evidence of any further NO_x descent in March possibly linked to the strengthening of the upper polar vortex. In 2011, ClONO₂ shows a slow and roughly constant decrease from January to March driven by the progressive decrease of the solar zenith angle, while upper stratospheric O₃ (around 1 hPa) remains about constant. In contrast, high ClONO₂ and O₃ values characterize the upper stratosphere in February 2009.

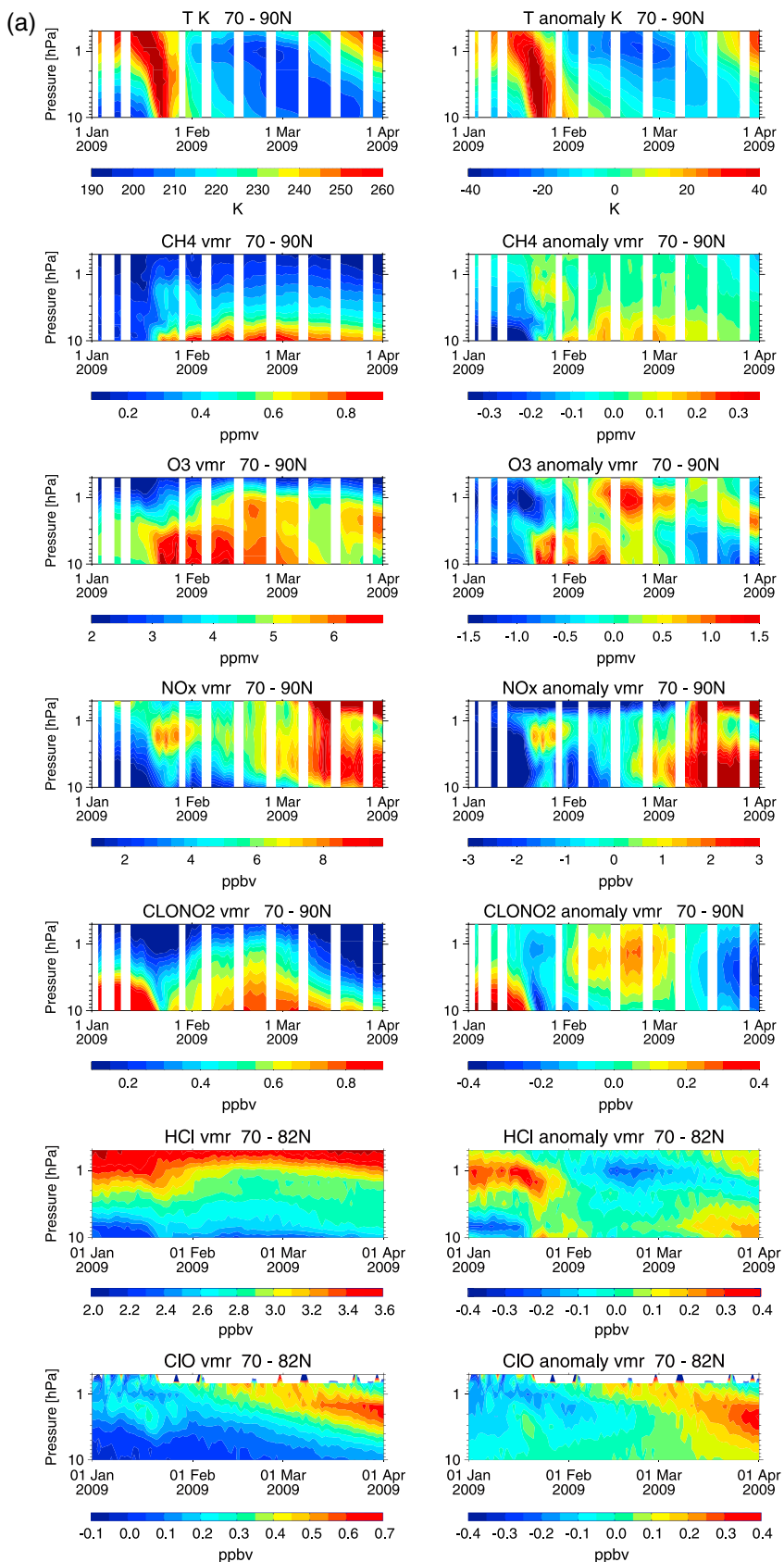


Figure 3

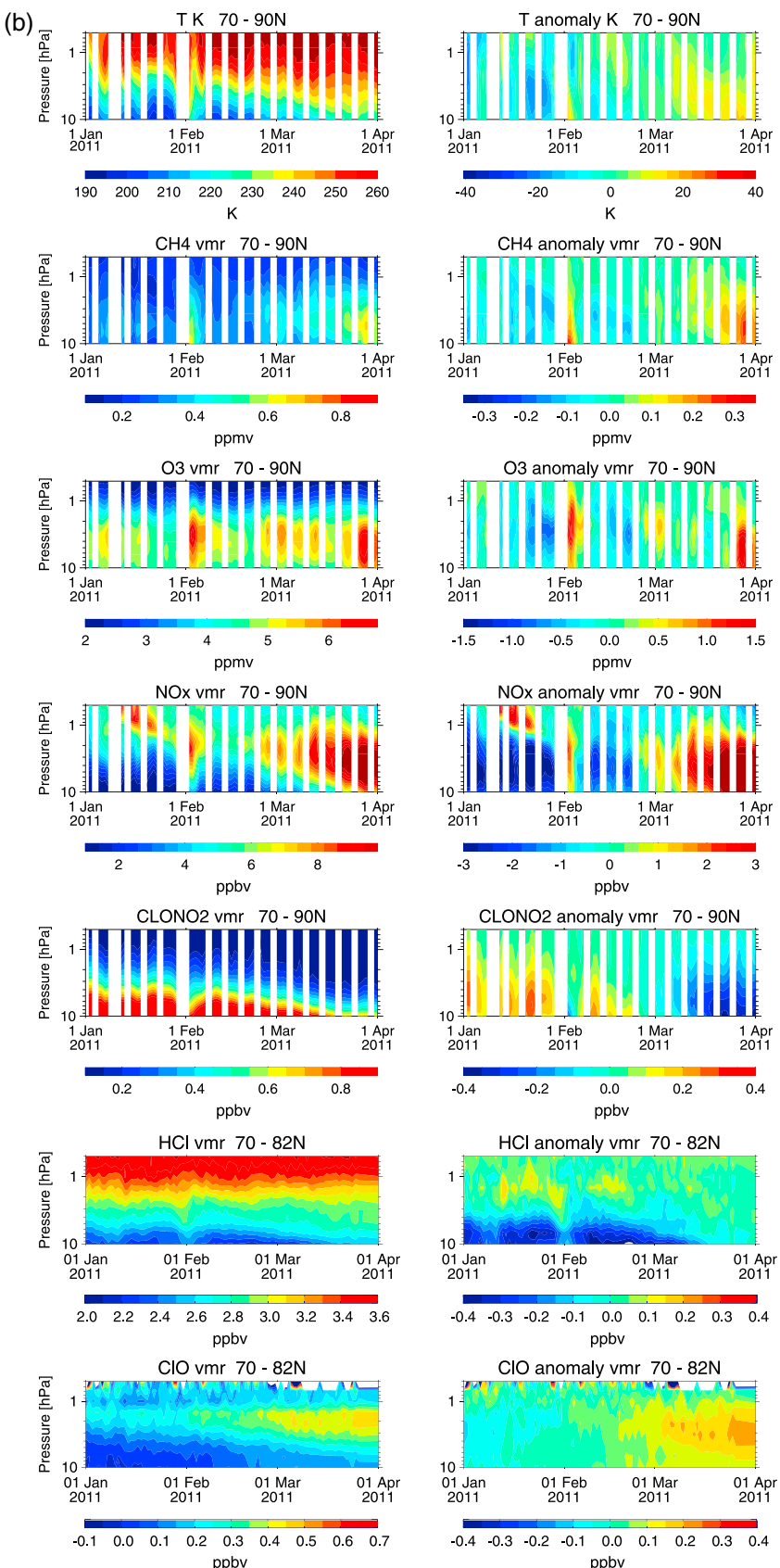


Figure 3. (continued)

The bottom rows of Figures 3a and 3b present the temporal evolution of 70–82°N zonal mean values and the anomalies in MLS HCl and ClO for January–March 2009 and 2011, respectively. An HCl decrease of up to about 0.4 ppbv is evident in February 2009, mainly between 2 and 0.5 hPa, hence roughly in the same region as the O₃ and ClONO₂ increases. *Damiani et al.* [2012a] showed that large decreases in HCl occurred in February 2006 and 2009 and that they were even larger than the variations induced by the solar proton events (SPEs) of January 2005. Moreover, unlike January 2005, when the enhancement in SPE-induced hydroxyl radicals caused an HCl decrease with the consequent HOCl increase, HCl reductions in February 2009 are not coupled with any changes in HOCl. The enhancement in active chlorine in the form of ClO is smaller in absolute values (see also Figure 6), but it is coupled with the almost simultaneous increase of ClONO₂.

On the other hand, only some minor variations in the upper stratospheric HCl are evident during February 2011, while the ClO concentration is generally lower than 2009 in particular in late February/March. Despite the fact that descending ClO isolines are visible in both 2009 and 2011 below about 1.5 hPa, the ClO distribution above this altitude is different. There, while no evident variability or seasonal trend are manifested in 2011, the 2009 anomaly time series show a progressive descent in the ClO enhancement, more apparent after the end of February, which overlap the usual ClO temporal evolution occurring at lower altitudes. The photolysis of ClONO₂ around 1.5 hPa caused by the gradual increase of the solar illumination offers an explanation to this. Clear differences in the temporal evolution of both HCl and ClO between 2009 and 2011 are then evident.

Figure 4 shows the geographic distribution (i.e., maps) of MIPAS temperature, CH₄, O₃, NO_x, and ClONO₂ on the 1700 K isentropic surface on 10 January (before the January SSW) and on 1, 12, and 21 February 2009 (after the SSW). After the SSW event, the upper stratospheric temperatures start to decrease and remain very low into late February. Air rich in CH₄ intrudes into the high latitudes soon after the SSW. Then, the low CH₄ values remain mostly confined north of 70°N, indicating a recovered polar vortex well centered over the North Pole. The very low NO_x VMRs, which define the inner polar vortex in January, slightly increase after the SSW and a more homogeneous latitudinal distribution characterized by higher NO_x abundance forms. Then, clues of the mesospheric NO_x descent are discernible at high latitudes on 21 February. While in the middle stratosphere, O₃ usually decreases with increasing latitudes, so that lower O₃ values are present in the polar vortex; differences are smaller at higher altitudes. Figure 4 shows a progressive enhancement in upper stratospheric O₃ in the polar vortex. O₃ abundances increase throughout the month of February, and the area characterized by elevated O₃ mirrors the region characterized by the low temperatures by the end of the month.

We recall that the reaction rate of the O₃ production reaction



is greater at lower temperatures. In contrast, the ozone loss reaction



is less effective at lower temperatures. Moreover, this temperature dependence also applies to the majority of the other bimolecular reactions destroying O₃ (e.g., NO + O₃) [Sonnenmann et al., 2006]. At steady state and assuming pure oxygen chemistry, the temperature dependence of the odd oxygen (O₃ + O) is dominated by the ozone sink reaction (R2). Therefore, the O₃ enhancement highlighted in Figures 3a and 4 is mostly due to the strong temperature decrease, mainly because of the temperature dependence of the odd oxygen loss reaction [Barnett et al., 1975; see also Jonsson et al., 2004].

The temperature dependence of the odd oxygen is related to the temperature influence of its destruction reaction via pure oxygen chemistry (i.e., reaction (R2)) but also to the different temperature dependences of HO_x, NO_x, and ClO_x destroying O₃ via catalytic cycles. Therefore, under photochemical equilibrium conditions,

Figure 3. (a) Temporal evolution of (left column) zonal mean values and (right column) differences with respect to the average of the January–March period in (top to bottom rows) MIPAS temperature, CH₄, O₃, NO_x, ClONO₂, and MLS HCl, ClO between 10 and 0.5 hPa for January–March 2009 at 70–90°N and 70–82°N, respectively. (b) Temporal evolution of zonal mean values in Figure 3 (left) and differences with respect to the average of the January–March period in Figure 3 (right) in MIPAS temperature, CH₄, O₃, NO_x, ClONO₂, and MLS HCl, ClO between 10 and 0.5 hPa for January–March 2011 at 70–90°N and 70–82°N, respectively.

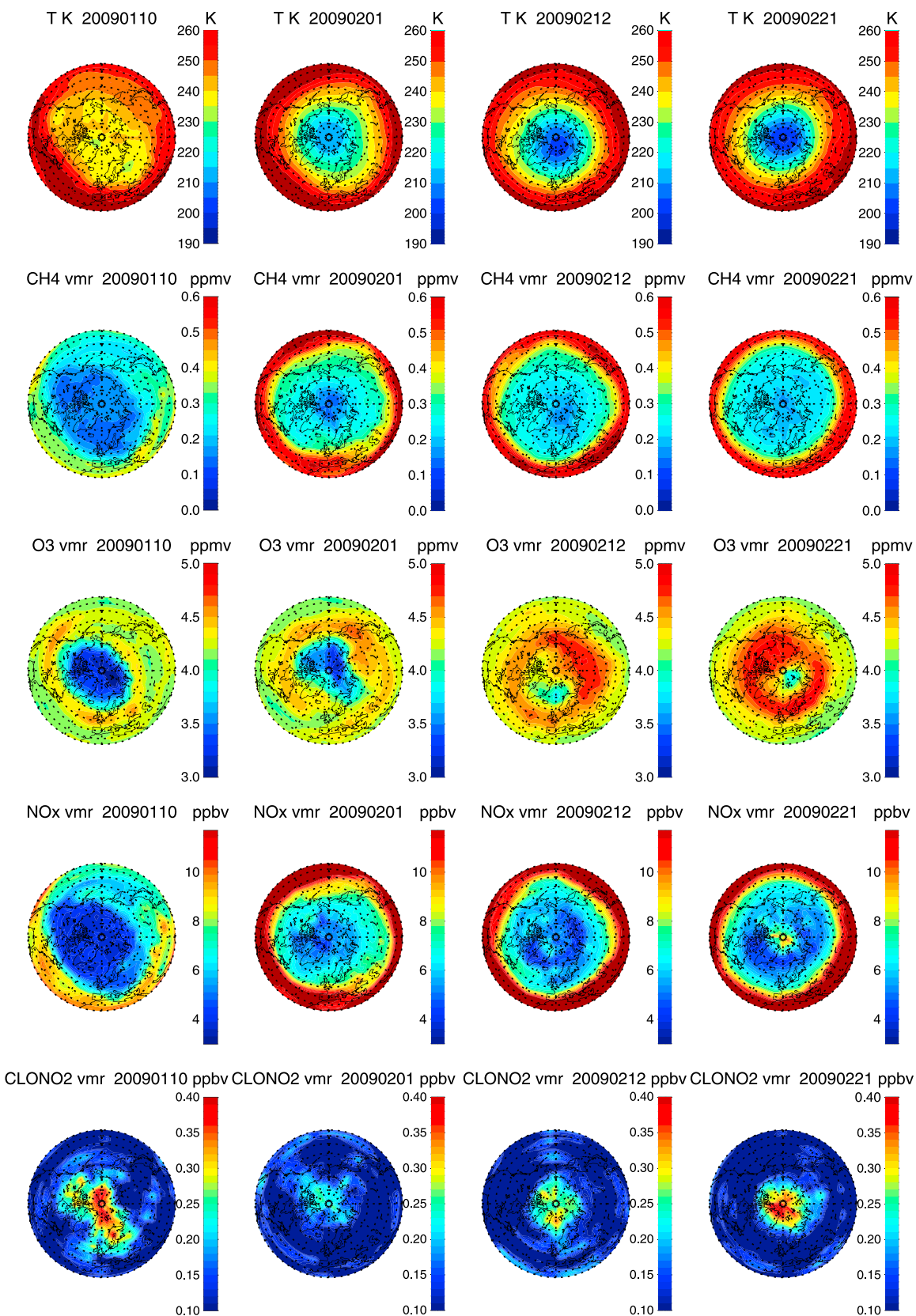


Figure 4. Geographic distribution of (top to bottom rows) MIPAS temperature, CH₄, O₃, NO_x, and ClONO₂ on the 1700 K isentropic surface (about 1.5 hPa) on (from left to right column) 10 January (before the January SSW) and on 1, 12, and 21 February 2009 (after the SSW).

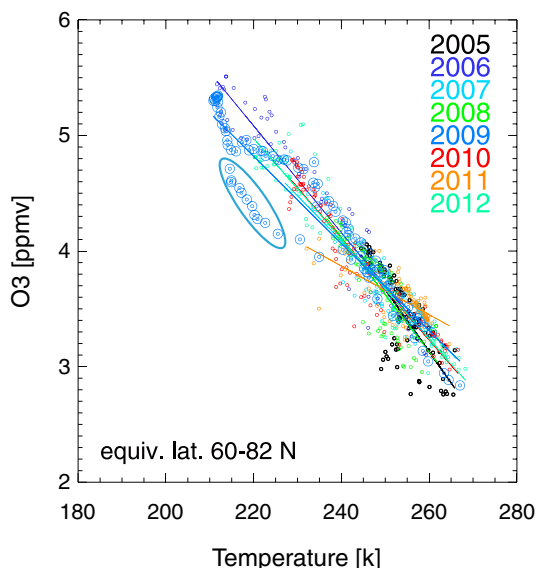


Figure 5. Scatterplots between MLS temperature and O₃ averaged over the equivalent latitudes 60–82°N at 1 hPa for January–March in 2005–2012. Linear regression lines are also shown. The double circles highlight the 2009 data. The oval line highlights the days characterized by the intrusion of midlatitude air to high latitudes in early February (see Figure 2).

February 2009 (see the temporal evolution of the CH₄ in Figure 2). These days correspond to the points highlighted in Figure 5. When these days are removed, the slope for 2009 (−0.041) becomes closer to the multiyear mean. Nevertheless, the mixing of the in-vortex air masses, influenced by different illumination conditions, provides an additional variability and makes difficult the interpretation of the results.

Despite the fact that we employed absolute values averaged over a large region affected by transport processes and over a long period of time, the slope of the regression lines is usually close to the results of Smith [1995] (see her Figure 9). Therefore, the inverse correlation between temperature and O₃ is also conserved inside the polar vortex, even if the vortex dynamics partially hide this. Both the 2006 and 2009 anomalous years are characterized by highest O₃ values in response to lowest temperatures. This suggests that the involved chemistry during the 2009 (and 2006) winter is similar to the other years.

The present study focused on the chemical changes that occurred around 1 hPa where the influence of NO_x catalytic cycle (highly temperature dependent) is expected to be small, while the region of the usual chlorine activation occurs at altitudes somewhat lower. Indeed, Figure 3 clearly shows that during the second half of February, the NO_x values are low in the region of enhanced O₃. On the other hand, the HO_x cycles could be relevant but only under sunshine conditions.

Overall, the effectiveness of the catalytic cycles on the presented O₃ variations in February is very limited because of the still prevailing nighttime conditions in the investigated region. In contrast, they are important in spring being the major reason of the sudden O₃ depletion occurring roughly below 2 hPa in mid-March (see Figure 3a). This interpretation is in agreement with a recent analysis based on the 3-D FinROSE chemistry transport model [Salmi et al., 2011].

the slope of the regression line between temperature and O₃ will experience different values for different seasons depending on the dominance of the different destruction paths [e.g., Barnett et al., 1975; Froidevaux et al., 1989; Smith, 1995]. Nevertheless, when applying this methodology to the present situation, the dynamics of the polar vortex tends to hide the T/O₃ relation at short time scale (e.g., weeks, results not shown). Therefore, we further tried to elucidate the influence of the temperature on O₃ by performing correlation analyses at longer time scales (i.e., months).

Figure 5 shows the scatterplot for MLS daily values of temperature and O₃ averaged over the equivalent latitudes 60–82°N at 1 hPa for January–March in 2005–2012. This region, representative of the polar vortex, usually presents high Pearson's correlation coefficient (*r*) values but also a consistent interannual variability due to the vortex dynamics (see Table 1). The slope of the regression line for 2009 (−0.038) is slightly lower than the multiyear mean slope (−0.046 ± 0.005, with both 2009 and 2011 excluded; see Table 1) and the slope of the other anomalous year (i.e., 2006). The intrusion of midlatitude air to high latitudes was particularly intense during early

Table 1. Pearson's Correlation Coefficient (*r*) and Slope of the Linear Regression Line Between MLS Temperature and O₃ Values Averaged Over the Equivalent Latitude 60–82°N at 1 hPa for January–March in 2005–2012

Year	2005	2006	2007	2008	2009	2010	2011	2012
<i>r</i>	−0.77	−0.97	−0.91	−0.82	−0.94	−0.95	−0.71	−0.97
Slope	−0.054	−0.046	−0.039	−0.049	−0.038	−0.044	−0.021	−0.043

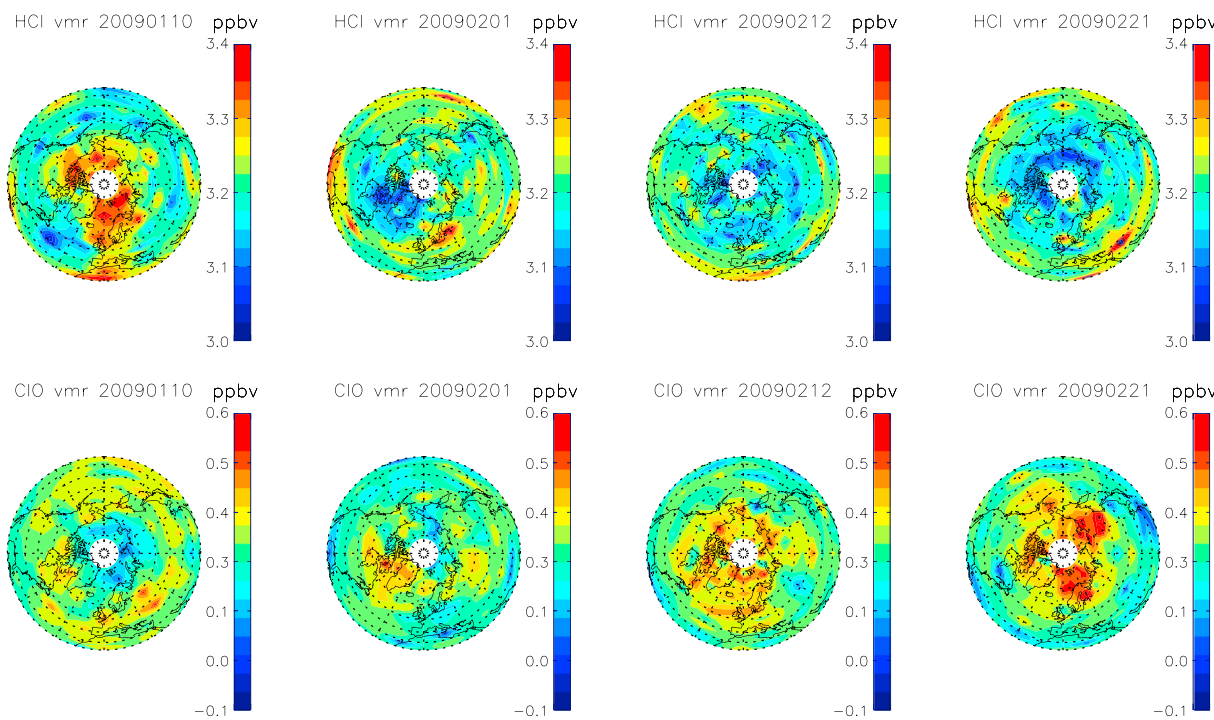


Figure 6. Geographic distribution of (top row) MLS HCl and (bottom row) ClO on the 1700 K isentropic surface (about 1.5 hPa) on (from left to right column) 10 January (before the January SSW) and on 1, 12, and 21 February 2009 (after the SSW).

It is also important to carefully examine the ClONO₂ variability during the investigated period. After the SSW event, it gradually increases until the maximum mixing ratios are reached in late February 2009 (see Figures 3a and 4). This gas is an important chlorine reservoir species during the winter polar night. Its formation depends on the availability of NO₂ and ClO as well as on air density as follows:



ClONO₂ is destroyed via photolysis by near-UV solar radiation, and usually its concentration peaks in the lower stratosphere. During strong SSW events, its concentration at high latitudes is expected to be reduced because of the mixing of ClONO₂-rich polar air with air from lower latitudes, where ClONO₂ has been photolyzed by UV radiation. Since the ClONO₂ formation depends on both ClO and NO₂ concentrations, it is remarkable to note that the ingress of the midlatitude air to the polar vortex during and after the SSW period did not result in a consistent variation of the NO_x budget in the vortex in February (Figure 2). Moreover, while MIPAS NO₂ VMRs (not shown) in January were higher than in February for both 2009 and 2011, the peak of the ClONO₂ enhancement occurred during the second half of February 2009. Therefore, NO₂ does not appear to be the main driver of the increased upper stratospheric ClONO₂ VMRs shown in Figures 3a and 4.

Sudden high values of ClONO₂ in the upper stratosphere can occur after the SPEs, mainly under polar night conditions [Lopez-Puertas et al., 2005]. This is due to the enhanced availability of active chlorine arising from HCl depletion [Damiani et al., 2009]. In our case, the altitude and the magnitude of the layer of high ClONO₂ developing in February 2009 are roughly comparable to those for the ClONO₂ enhancement, which occurred after the SPE of October–November 2003 [Funke et al., 2011].

The geographic distribution of HCl on the 1700 K isentropic surface is shown in the top row of Figure 6. A progressive decrease of HCl occurs in February 2009, and it reaches the lowest values during the second half of the month when low HCl VMRs are mainly north of 70°N. Although measured with a different satellite instrument and with different altitude resolution (see section 2), in February, the geographic distribution of ClONO₂ (see Figure 4) seems to be linked to the HCl decrease and suggests a relationship between the temporal evolutions of the two compounds via ClO. However, due to the different local times at which the different satellite observations are recorded (see section 2), a perfect match between the

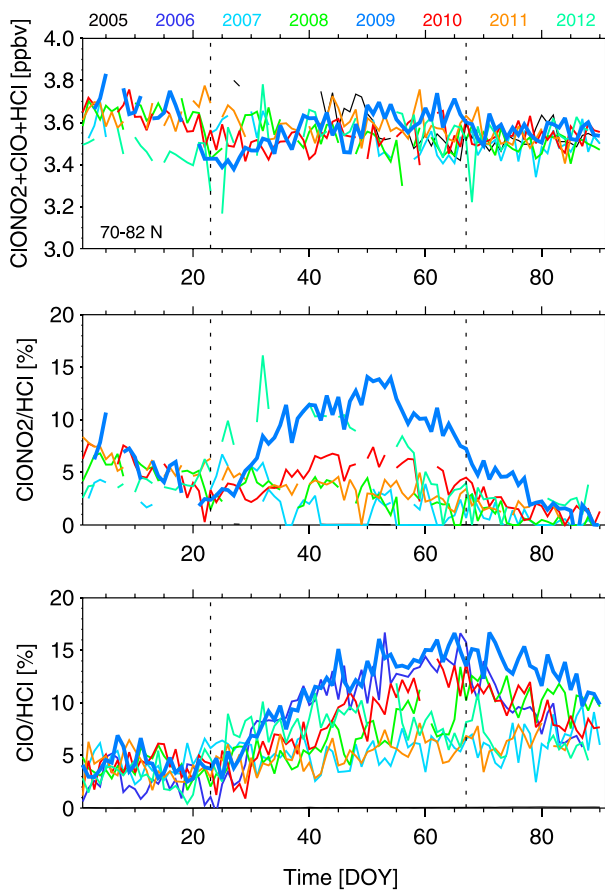


Figure 7. Time evolution of (top) the sum of VMRs of $\text{ClONO}_2 + \text{ClO} + \text{HCl}$, (middle) the ratio $\text{ClONO}_2/\text{HCl}$, and (bottom) the ratio ClO/HCl calculated from MLS and MIPAS profiles at 1 hPa averaged over the latitudinal band $70\text{--}82^\circ\text{N}$ for 2005–2012. The vertical dashed lines show the occurrence of the SPEs of January and March 2012.

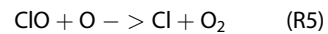
[e.g., Brasseur and Solomon, 2005; Siskind et al., 1998]. Then, reaction (R3) allows ClONO_2 formation mainly below 1 hPa (see Figures 3a and 4). Nevertheless, it is interesting to note that while the strongest variation in O_3 and HCl occurs at 1 hPa, the correspondent peaks in ClO and ClONO_2 seem to be slightly moved above and below this altitude, respectively.

In order to analyze the development of the chlorine partitioning, the sum of VMRs of $\text{ClONO}_2 + \text{ClO} + \text{HCl}$ was computed from MLS and MIPAS profiles at 1 hPa averaged over the latitudinal band $70\text{--}82^\circ\text{N}$ for 2005–2012 and presented in Figure 7 (top). Moreover, Figure 7 (middle and bottom) show the ratio of $\text{ClONO}_2/\text{HCl}$ and ClO/HCl , respectively. While during the period of the SSW of January 2009, the sum of $\text{ClONO}_2 + \text{ClO} + \text{HCl}$ presents the lowest values (about 3.4 ppbv), since about 10 February, the VMRs remain almost constant. This confirms our previous findings and justifies confidence in our data set. Moreover, it is worth noting that the sum of the VMRs for 2009 is approximately equal to the other years. This excludes that the observed anticorrelation of ClONO_2 and HCl perturbations at polar latitudes could be influenced by the in-mixing of lower latitude air.

Both $\text{ClONO}_2/\text{HCl}$ and ClO/HCl reach about 15% in 2009; nevertheless, the former peaks in mid-February while the latter in early March. The decreasing trend of the sum of the chlorine VMRs during January 2009 seems to be mainly driven by a reduction in high-latitude ClONO_2 abundance. This was caused by the mixing of polar air with air with low ClONO_2 VMRs from lower latitudes (during/after the SSW) and by photolysis processes (before the SSW) occurred because of the distorted polar vortex. The ClO/HCl ratio for 2006 is very close to the 2009 values in February, while it is smaller in March. No ClONO_2 MIPAS data are available for the 2006 winter.

two data sets is not expected. The bottom row of Figure 6 shows the CIO maps on the 1700 K isentropic surface. Even if MLS CIO is rather noisy [Santee et al., 2008], there is a general increasing trend in CIO in February, pointing to the ongoing change in the chlorine partitioning.

In the middle/lower stratosphere, daytime ClO_x ($\text{Cl} + \text{ClO}$) is mainly in the form of ClO , while the ratio Cl/ClO increases up to about 0.9 around 55 km [e.g., Ricaud et al., 2000]. At short time scales, the evolution of ClO is governed by the partitioning within ClO_x as follows:



Therefore, the ClO/Cl ratio depends on the O_3/O partitioning. Because at steady state the rate of creation of ozone from three body collisions equals the rate of photodissociation of ozone by sunlight, in addition to the above mentioned enhancement in the odd oxygen driven by reaction (R2), the very low temperatures of February 2009 favor a shift in the ratio of O_3/O toward O_3 (see reaction (R1)) and hence ClO . HCl is the main chlorine reservoir in the stratosphere. Since the reaction of Cl with CH_4 and HO_x leads to the sequestering of reactive chlorine in HCl , changes in the partitioning within ClO_x in favor of ClO will decrease HCl

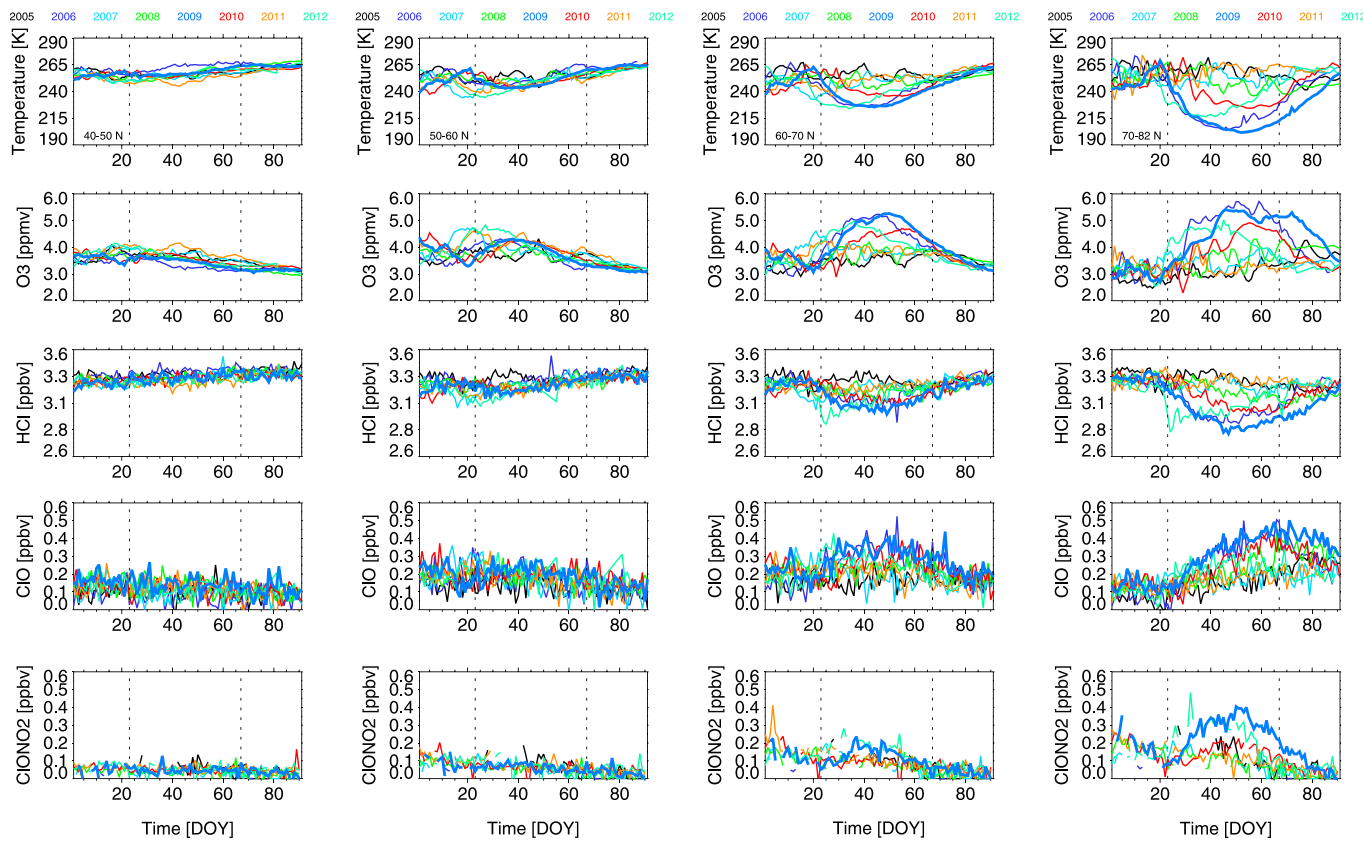


Figure 8. Time evolution of (top to bottom) zonal mean temperature, O₃, HCl, ClO, and ClONO₂ at 1 hPa averaged over the latitudinal band 40–50°N, 50–60°N, 60–70°N, and 70–82°N as observed by MLS and MIPAS for 2005–2012. The vertical dashed lines show the occurrence of the SPEs of January and March 2012.

Figure 8 shows the time evolution of (top to bottom) zonal mean temperature, O₃, HCl, ClO, and ClONO₂ at 1 hPa averaged over four different latitudinal bands (i.e., 40–50°, 50–60°, 60–70°, and 70–82°) as observed by MLS and MIPAS for 2005–2012. Despite the fact that the majority of recent winters were characterized by SSW events leading to consequent atypical evolution of the gas species, 2006 and 2009 still stand out as anomalous. The temporal evolution of the temperature and gases is latitude dependent, so changes at lower latitudes last less time and have a smaller intensity compared with the variations occurring at high latitudes. Moreover, while variations in ClONO₂ occur only at very high latitudes, changes affecting the other compounds are clearly discernible also at 50–60°N.

Temperature is the main driver of these composition changes. For example, at latitudes greater than 60–70°N, the record low values of temperature last longer in February–March 2009 with respect to the other years and are coupled with the strongest enhancements in O₃ and record high (low) values in ClO (HCl). Since in this period the westerlies recovered (Figure 1) and a consequent newly isolated polar vortex formed, horizontal transport of low-latitude air cannot be the main driver of these changes during 2009.

An additional interesting feature arising from Figure 8 is the sudden HCl decrease that occurred in January and March 2012, corresponding to the strong SPE events recently described by *von Claramann et al.* [2013] and *Jackman et al.* [2014]. The January 2012 event occurred under SSW conditions, and the resulting chemical changes are a combination of both effects [*Päivärinta et al.*, 2013]. Following the chemical paths already described above, also in January 2012 SPE-driven enhancements in hydroxyl radicals caused HCl depletion. The consequent simultaneous chlorine activation was mainly in the form of an intense short-term HOCl increase of about 0.4 ppbv [*Damiani et al.*, 2012b]. These short-term SPE effects are superimposed on the large-scale subsidence of mesospheric air, which partly masks direct chemical SPE effects [*von Claramann et al.*, 2013]. Therefore, the combination of both SPE and SSW effects caused a sudden decrease in HCl VMRs, keeping its concentration low for a long period. This superimposition of effects impacted also NO_x and O₃ [*Päivärinta et al.*, 2013].

4. Conclusions

We have shown that the SSW, which occurred on 24 January 2009, had a major influence on the composition of the northern polar upper stratosphere and lower mesosphere by triggering strong temperature variations in February. Record high values of O₃, ClO, and ClONO₂ coupled to record low values of temperature and HCl for the winters of 2005–2012 have been measured in February 2009. ClO_x was repartitioned toward ClO. This allowed an increased anomalous formation of ClONO₂ lasting until the enhanced photolysis of ClONO₂ took place in March. The temporal development of the ozone distributions appears to be explained by the temperature dependence of the ozone loss reactions, while the repartitioning of ClO_x toward ClO is a consequence of the shift in the O₃/O ratio toward O₃, mainly driven by the temperature dependence of the reaction of the O₃ production.

Additional correlation analysis performed between temperature and O₃ showed that the expected anticorrelation is more evident for long time scales (i.e., months), while the vortex dynamics tends to hide it for shorter time scales. The horizontal air mixing between polar and midlatitude air is evident mostly between the SSW occurrence and the early February 2009, and it is characterized by the ingress of higher CH₄ VMRs and by a small reduction (about 0.2 ppbv) of the sum of VMRs of ClONO₂ + ClO + HCl to high latitudes. In contrast, during the period after about 10 February, despite the intense ongoing chlorine partitioning, the sum of VMRs roughly remains constant and similar to the usual year-to-year variability.

Although the northern polar atmosphere in February 2009 was characterized by an elevated stratopause event, the investigated region is not influenced by the descent of mesospheric air rich in NO_x. Only limited enhancements in NO_x at ~1 hPa are discernible at latitudes greater than 80°N after 20 February, but they did not substantially affect O₃ and ClONO₂ in February.

Overall, since the investigated chemical changes occurred mostly under nighttime conditions, we can exclude a driving influence from the catalytic cycles on the O₃ variation, while they are important in explaining its depletion in middle March.

Such processes have not been observed in 2011, during which the stratospheric polar vortex was mostly isolated and stable. Similar atypical chemical conditions occurred also in February 2006, but 2009 still stands out for the persistence of its effects, remaining perturbed until late March.

Acknowledgments

The support of USACH-DICYT, FONDEF (IT13I10034), and FONDECYT (1140239) is gratefully acknowledged. A.D. was also supported by the SOUSEI program, MEXT, JAPAN. Work at the Jet Propulsion Laboratory, California Institute of Technology, was done under contract with NASA. The IAA team was supported by the Spanish MCINN under grant AYA2011-23552 and EC FEDER funds. IMK/IAA-generated MIPAS/Envisat data can be obtained by registered users from the data server: <http://www.imk-asf.kit.edu/english/308.php>. MLS/Aura data are available at the Jet Propulsion Laboratory MLS website: <http://mls.jpl.nasa.gov/index.php>.

References

- Baldwin, M. P., and T. J. Dunkerton (2001), Stratospheric harbingers of anomalous weather regimes, *Science*, 244, 581–584.
- Barnett, J. J., J. T. Houghton, and J. A. Pyle (1975), The temperature dependence of the ozone concentration near the stratopause, *Q. J. R. Meteorol. Soc.*, 101, 245–257.
- Brasseur, G., and S. Solomon (2005), *Aeronomy of the Middle Atmosphere 3rd Revised and Enlarged*, Springer, Dordrecht, Netherlands.
- Charlton-Perez, A. J., L. M. Polvani, J. Austin, and F. Li (2008), The frequency and dynamics of stratospheric sudden warmings in the 21st century, *J. Geophys. Res.*, 113, D16116, doi:10.1029/2007JD009571.
- Damiani, A., P. Diego, M. Laurenza, M. Storini, and C. Rafanelli (2009), Ozone variability related to several SEP events occurring during solar cycle no. 23, *Adv. Space Res.*, 43, 28–40.
- Damiani, A., M. Storini, M. L. Santee, and S. Wang (2010), Variability of the nighttime OH layer and mesospheric ozone at high latitudes during northern winter: Influence of meteorology, *Atmos. Chem. Phys.*, 10, 10,291–10,303, doi:10.5194/acp-10-10291-2010.
- Damiani, A., et al. (2012a), Impact of January 2005 solar proton events on chlorine species, *Atmos. Chem. Phys.*, 12, 4159–4179, doi:10.5194/acp-12-4159-2012.
- Damiani, A., et al. (2012b), Effects of January 2005 SPEs on the chemistry of the polar atmosphere, Japan Geoscience Union Meeting 2012, Chiba, Japan.
- Douglass, A. R., R. S. Stolarski, S. E. Strahan, and L. D. Oman (2012), Understanding differences in upper stratospheric ozone response to changes in chlorine and temperature as computed using CCMVal-2 models, *J. Geophys. Res.*, 117, D16306, doi:10.1029/2012JD017483.
- Fischer, H., et al. (2008), MIPAS: An instrument for atmospheric and climate research, *Atmos. Chem. Phys.*, 8, 2151–2188, doi:10.5194/acp-8-2151-2008.
- Froidevaux, L., M. Allen, S. Berman, and A. Daughton (1989), The mean ozone profile and its temperature sensitivity in the upper stratosphere and lower mesosphere: An analysis of LIMS observations, *J. Geophys. Res.*, 94(D5), 6389–6417, doi:10.1029/JD094iD05p06389.
- Froidevaux, L., et al. (2008a), Validation of Aura Microwave Limb Sounder HCl measurements, *J. Geophys. Res.*, 113, D15S25, doi:10.1029/2007JD009025.
- Froidevaux, L., et al. (2008b), Validation of Aura Microwave Limb Sounder stratospheric ozone measurements, *J. Geophys. Res.*, 113, D15S20, doi:10.1029/2007JD008771.
- Funke, B., M. López-Puertas, D. Bermejo-Pantaleón, M. García-Comas, G. P. Stiller, T. von Clarmann, M. Kiefer, and A. Linden (2010), Evidence for dynamical coupling from the lower atmosphere to the thermosphere during a major stratospheric warming, *Geophys. Res. Lett.*, 37, L13803, doi:10.1029/2010GL043619.
- Funke, B., et al. (2011), Composition changes after the “Halloween” solar proton event: The High-Energy Particle Precipitation in the Atmosphere (HEPPA) model versus MIPAS data intercomparison study, *Atmos. Chem. Phys. Discuss.*, 11, 9407–9514, doi:10.5194/acpd-11-9407-2011.

- Gao, H., J. Xu, W. Ward, and A. K. Smith (2011), Temporal evolution of nightglow emission responses to SSW events observed by TIMED/SABER, *J. Geophys. Res.*, **116**, D19110, doi:10.1029/2011JD015936.
- Gille, J. C., G. P. Anderson, W. J. Kohri, and P. L. Bailey (1981), Observations of the interaction of ozone and dynamics, in *Proceedings of the Quadrennial International Ozone Symposium, 4–9 August 1980*, edited by J. London, pp. 1007–1011, Int. Assoc. of Meteorol. and Atmos. Phys., Boulder, Colo.
- Hauchecorne, A., et al. (2010), Response of tropical stratospheric O₃, NO₂ and NO₃ to the equatorial Quasi-Biennial Oscillation and to temperature as seen from GOMOS/ENVISAT, *Atmos. Chem. Phys.*, **10**, 8873–8879, doi:10.5194/acp-10-8873-2010.
- Holton, J. R. (1983), The influence of gravity wave breaking on the general circulation of the middle atmosphere, *J. Atmos. Sci.*, **40**, 2497–2507.
- Höpfner, M., et al. (2007), Validation of MIPAS CIONO₂ measurements, *Atmos. Chem. Phys.*, **7**, 257–281, doi:10.5194/acp-7-257-2007.
- Jackman, C. H., C. E. Randall, V. L. Harvey, S. Wang, E. L. Fleming, M. López-Puertas, B. Funke, and P. F. Bernath (2014), Middle atmospheric changes caused by the January and March 2012 solar proton events, *Atmos. Chem. Phys.*, **14**, 1025–1038, doi:10.5194/acp-14-1025-2014.
- Jonsson, A. I., J. de Grandpré, V. I. Fomichev, J. C. McConnell, and S. R. Beagley (2004), Doubled CO₂-induced cooling in the middle atmosphere: Photochemical analysis of the ozone radiative feedback, *J. Geophys. Res.*, **109**, D24103, doi:10.1029/2004JD005093.
- Kvissel, O.-K., Y. J. Orsolini, F. Stordal, V. Limpasuvan, J. Richter, and D. R. Marsh (2012), Mesospheric intrusion and anomalous chemistry during and after a major stratospheric sudden warming, *J. Atmos. Sol. Terr. Phys.*, **78**–**79**, 116–124, doi:10.1016/j.jastp.2011.08.015.
- Livesey, N. J., et al. (2011), Earth Observing System (EOS) Microwave Limb Sounder (MLS) Version 3.3 Level 2 data quality and description document, *Rep. JPL D-33509*, Version 3.3x-1.0, Jet Propul. Lab., Calif. Inst. of Technol., Pasadena.
- Lopez-Puertas, M., B. Funke, S. Gil-Lopez, T. von Clarmann, G. P. Stiller, M. Hopfner, S. Kellmann, G. Mengistu Tsidu, H. Fischer, and C. H. Jackman (2005), HNO₃, N₂O₅ and CIONO₂ enhancements after the October–November 2003 solar proton events, *J. Geophys. Res.*, **110**, A09S44, doi:10.1029/2005JA011051.
- Manney, G. L., et al. (2008a), The evolution of the stratopause during the 2006 major warming: Satellite data and assimilated meteorological analyses, *J. Geophys. Res.*, **113**, D11115, doi:10.1029/2007JD009097.
- Manney, G. L., et al. (2008b), The high Arctic in extreme winters: Vortex, temperature, and MLS and ACE-FTS trace gas evolution, *Atmos. Chem. Phys.*, **8**, 505–522, doi:10.5194/acp-8-505-2008.
- Manney, G. L., M. J. Schwartz, K. Krüger, M. L. Santee, S. Pawson, J. N. Lee, W. H. Daffer, R. A. Fuller, and N. J. Livesey (2009), Aura Microwave Limb Sounder observations of dynamics and transport during the record-breaking 2009 Arctic stratospheric major warming, *Geophys. Res. Lett.*, **36**, L12815, doi:10.1029/2009GL038586.
- Manney, G. L., et al. (2011), Unprecedented Arctic ozone loss in 2011, *Nature*, **478**, 469–475, doi:10.1038/nature10556.
- Matsuno, T. (1971), A dynamical model of the stratospheric sudden warming, *J. Atmos. Sci.*, **28**, 1479–1494.
- Nash, E. R., P. A. Newmann, J. E. Rosenfield, and M. R. Schoeberl (1996), An objective determination of the polar vortex using Ertel's potential vorticity, *J. Geophys. Res.*, **101**, 9471–9478, doi:10.1029/96JD00066.
- Orsolini, Y. J., J. Urban, D. P. Murtagh, S. Lossow, and V. Limpasuvan (2010), Descent from the polar mesosphere and anomalously high stratopause observed in 8 years of water vapor and temperature satellite observations by the Odin sub-millimeter radiometer, *J. Geophys. Res.*, **115**, D12305, doi:10.1029/2009JD013501.
- Päiväranta, S.-M., A. Seppälä, M. E. Andersson, P. T. Verronen, L. Thölix, and E. Kyrölä (2013), Observed effects of solar proton events and sudden stratospheric warmings on odd nitrogen and ozone in the polar middle atmosphere, *J. Geophys. Res. Atmos.*, **118**, 6837–6848, doi:10.1002/jgrd.50486.
- Randall, C. E., V. L. Harvey, C. S. Singleton, P. F. Bernath, C. D. Boone, and J. U. Kozyra (2006), Enhanced NO_x in 2006 linked to upper stratospheric Arctic vortex, *Geophys. Res. Lett.*, **33**, L18811, doi:10.1029/2006GL027160.
- Randall, C. E., V. L. Harvey, D. E. Siskind, J. France, P. F. Bernath, C. D. Boone, and K. A. Walker (2009), NO_x descent in the Arctic middle atmosphere in early 2009, *Geophys. Res. Lett.*, **36**, L18811, doi:10.1029/2009GL039706.
- Ricaud, P., M. P. Chipperfield, J. W. Waters, J. M. Russell, and A. E. Roche (2000), Temporal evolution of chlorine monoxide in the middle stratosphere, *J. Geophys. Res.*, **105**, 4459–4469, doi:10.1029/1999JD900995.
- Rood, R. B., and A. R. Douglass (1985), Interpretation of ozone temperature correlations 1. Theory, *J. Geophys. Res.*, **90**, 5733–5743, doi:10.1029/JD090iD03p05733.
- Salmi, S.-M., P. T. Verronen, L. Thölix, E. Kyrölä, L. Backman, A. Y. Karpechko, and A. Seppälä (2011), Mesosphere-to-stratosphere descent of odd nitrogen in February–March 2009 after sudden stratospheric warming, *Atmos. Chem. Phys.*, **11**, 4645–4655, doi:10.5194/acp-11-4645-2011.
- Santee, M. L., et al. (2008), Validation of the Aura Microwave Limb Sounder ClO measurements, *J. Geophys. Res.*, **113**, D15S22, doi:10.1029/2007JD008762.
- Schwartz, M. J., et al. (2008), Validation of the Aura Microwave Limb Sounder temperature and geopotential height measurements, *J. Geophys. Res.*, **113**, D15S11, doi:10.1029/2007JD008783.
- Sinnhuber, B.-M., G. Stiller, R. Ruhnke, T. von Clarmann, S. Kellmann, and J. Aschmann (2011), Arctic winter 2010/2011 at the brink of an ozone hole, *Geophys. Res. Lett.*, **38**, L24814, doi:10.1029/2011GL049784.
- Siskind, D. E., L. Froidevaux, J. M. Russell, and J. Lean (1998), Implications of upper stratospheric trace constituent changes observed by HALOE for O₃ and ClO from 1992 to 1995, *J. Geophys. Res.*, **25**(18), 3513–3516.
- Siskind, D. E., S. D. Eckermann, L. Coy, J. P. McCormack, and C. E. Randall (2007), On recent interannual variability of the Arctic winter mesosphere: Implications for tracer descent, *Geophys. Res. Lett.*, **34**, L09806, doi:10.1029/2007GL029293.
- Smith, A. K. (1995), Numerical simulation of global variations of temperature, ozone, and trace species in the stratosphere, *J. Geophys. Res.*, **100**, 1253–1269, doi:10.1029/94JD02395.
- Smith, A. K., M. Lopez-Puertas, M. Garcia-Comas, and S. Tukiainen (2009), SABER observations of mesospheric ozone during NH late winter 2002–2009, *Geophys. Res. Lett.*, **36**, L23804, doi:10.1029/2009GL040942.
- Sofieva, V. F., N. Kalakoski, P. T. Verronen, S.-M. Päiväranta, E. Kyrölä, L. Backman, and J. Tamminen (2012), Polar-night O₃, NO₂ and NO₃ distributions during sudden stratospheric warmings in 2003–2008 as seen by GOMOS/EnviroSat, *Atmos. Chem. Phys.*, **12**, 1051–1066, doi:10.5194/acp-12-1051-2012.
- Sonnemann, G. R., M. Grygalashvily, and U. Berger (2006), Impact of a stratospheric warming event in January 2001 on the minor constituents in the MLT region calculated on the basis of a new 3-D-model LIMA of the dynamics and chemistry of the middle atmosphere, *J. Atmos. Sol. Terr. Phys.*, **68**, 2012–2025.
- Stolarski, R. S., A. R. Douglass, E. E. Remsberg, N. J. Livesey, and J. C. Gille (2012), Ozone temperature correlations in the upper stratosphere as a measure of chlorine content, *J. Geophys. Res.*, **117**, D10305, doi:10.1029/2012JD017456.
- Tomikawa, Y., K. Sato, S. Watanabe, Y. Kawatani, K. Miyazaki, and M. Takahashi (2012), Growth of planetary waves and the formation of an elevated stratopause after a major stratospheric sudden warming in a T213L256 GCM, *J. Geophys. Res.*, **117**, D16101, doi:10.1029/2011JD017243.

- Tweedy, O. V., et al. (2013), Nighttime secondary ozone layer during major stratospheric sudden warmings in specified-dynamics WACCM, *J. Geophys. Res. Atmos.*, 118, 8346–8358, doi:10.1002/jgrd.50651.
- von Clarmann, T., et al. (2003), Retrieval of temperature and tangent altitude pointing from limb emission spectra recorded from space by the Michelson Interferometer for Passive Atmospheric Sounding (MIPAS), *J. Geophys. Res.*, 108(D23), 4736, doi:10.1029/2003JD003602.
- von Clarmann, T., et al. (2009), Retrieval of temperature, H₂O, O₃, HNO₃, CH₄, N₂O, ClONO₂ and ClO from MIPAS reduced resolution nominal mode limb emission measurements, *Atmos. Meas. Tech.*, 2, 159–175, doi:10.5194/amt-2-159-2009.
- von Clarmann, T., B. Funke, M. López-Puertas, S. Kellmann, A. Linden, G. P. Stiller, C. H. Jackman, and V. L. Harvey (2013), The solar proton events in 2012 as observed by MIPAS, *Geophys. Res. Lett.*, 40, 464–469, doi:10.1002/grl.50119.
- Waters, J. W., et al. (2006), The Earth Observing System Microwave Limb Sounder (EOS MLS) on the Aura satellite, *IEEE T. Geosci. Remote*, 44, 1075–1092.
- Winick, J. R., P. P. Wintersteiner, R. H. Picard, D. Esplin, M. G. Mlynczak, J. M. Russell III, and L. L. Gordley (2009), OH layer characteristics during unusual boreal winters of 2004 and 2006, *J. Geophys. Res.*, 114, A02303, doi:10.1029/2008JA013688.